

# Three-dimensional reconstruction of single particle electron microscopy: the voltage sensitive sodium channel structure

YUTAKA UENO<sup>1</sup> AND CHIKARA SATO<sup>2</sup>

*Single particle analysis in electron microscopy allows direct observation of the reconstructed three-dimensional structures of protein molecules. This method enables a more comprehensive study of membrane proteins which have been problematic in structural studies using X-ray crystallography. These membrane proteins include the voltage-sensitive ion channel proteins, which play an important role in neural activities, and have great medical significance. The method described is supported by the development of cryo-electron microscopy and the angular reconstitution method. This review summarizes certain principles governing single particle analysis employing angular reconstitution. This method was applied to our study of the voltage-sensitive sodium channel, and the results are discussed. With improvements in resolutions and statistical analyses, the single particle technique is considered to be advantageous in studies of the structural changes and molecular interactions of protein molecules.*

## Introduction

Single particle analysis is a method for determining the structure of proteins and biological macromolecules using statistics based on direct observation by electron microscopy. While atomic structures derived from the crystallographic analysis of protein molecules render details of physical events in proteins, molecular shapes and envelopes revealed by electron microscopy provide biological insights into their structural change and interaction with other proteins.

---

<sup>1</sup>Computational Biology Research Center, and <sup>2</sup>Neuroscience Research Institute, National Institute of Advanced Industrial Science and Technology AIST Tsukuba Central 6, Tsukuba, 305-8566 Japan. Tel: (81) 298-61-5562; Fax: (81) 298-61-6482;  
E-mail: ti-sato@aist.go.jp

Beyond the observed images of microscopy, three-dimensional (3D) reconstruction by electron microscopy has also been established. This work has been pioneered by studies of helical assemblies of macromolecules<sup>1</sup> and two-dimensional protein crystals<sup>2</sup>, since the arrangements of those specimen amplify necessary signals for reconstructions using noisy images. Nowadays, numerous reconstructions of single particles have been reported, such as icosahedral viruses<sup>3</sup>, ribosome complex<sup>4,5</sup>, and isolated protein molecules. At present, cryo-electron microscopy using ice embedded specimens in a holey grid provides high resolution images minimizing radiation damage and background from the carbon base<sup>6</sup>. This direct imaging of freeze-trapped conformations of proteins provides advanced structural information regarding biological mechanisms. Furthermore, this techniques also allows crystallographic analysis by electron microscopy at atomic-level resolution.

While the crystallization of protein requires a substantial amount of protein, at almost visible levels, single particle analysis usually requires ten to hundreds of times of lesser amounts. Furthermore, specimens are exempt from special preparations, such as crystallization. Proteins have evolved in a manner dedicated to particular species and organisms, and thus belong to protein families sharing the same properties and characteristics. Unfortunately, some families are difficult to purify and crystallize. Consequently, single particle analysis has been employed in various studies of proteins which have been problematic to crystallize. In particular, the illustration of membrane proteins such as calcium release channel<sup>7</sup>, sodium channel<sup>8</sup>, calcium channel<sup>9</sup>, potassium channel<sup>10</sup> have provided further understanding of protein architecture even though their resolution is less than the atomic model. These proteins include the voltage sensitive channel, which is the main participant in neural excitations. Nevertheless, several membrane proteins including functionally important channels have been studied by crystallography using truncated proteins engineered to form a crystal by mutation. Recently, an atomic model of bacteria K channel has been established by means of X-ray crystallography<sup>11</sup>.

In this review, we focus first on the angular reconstitution method developed by van Heel under the condition of particle suspension with random orientations<sup>5</sup>. After providing an overview of electron microscopy, the principle and image processing procedure of the angular reconstitution are described. Our results regarding the voltage sensitive sodium channel protein are then summarized in the following sections. For more details about electron microscopy and 3D reconstruction see refs 12 and 13. We also discuss practical

computer programs and necessary developments in the modern computational environment.

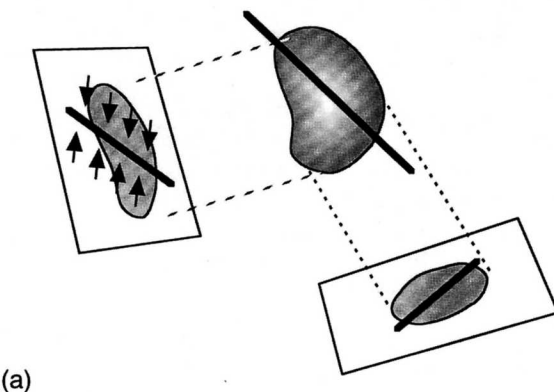
## Imaging in electron microscopy

In transmission electron microscopy (TEM), the projection image is formed by irradiating the specimen with a beam of electrons. They are scattered by the atomic Coulomb potential of the specimen, and they are focused into an image which is magnified more than 10,000 times by the electric lens system. The physical events taking place between the specimen and electrons are rather complex; however, the imaging works as a structure projector of the particle when the majority of the scattering is elastic<sup>12</sup>. Using a coherent field emission gun with an acceleration voltage of 50–300 kV, the following conditions are employed in order to minimize damage to the biological specimens.

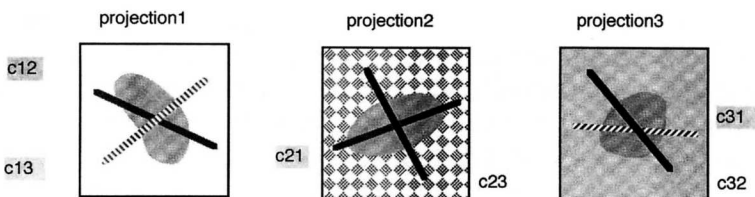
Cryo-electron microscopy has been invented to observe unfixed, unstained, and unsupported suspended protein samples and biological macromolecules<sup>14</sup>. By cooling the specimen close to absolute zero, radiation damage is minimized. With quick freezing of the suspension of the particles before the formation of ice crystals, the frozen-hydrated biological particles are expected to present a native structure. Therefore, the specimens are prepared by cooling its suspension into vitreous thin ice layers on a holey carbon grid. The specimen is then observed during its cooling stage by means of electron microscopy using an electron dose low enough to avoid damage and water evaporation. This technology was developed in crystal specimens allowing diffraction at atomic resolution, where the radiation damage was decreased up to 20 times<sup>6</sup>.

Negative staining is a popular technique because of its practical feasibility using standard equipment. It produces a reverse contrast in the biological specimens through the use of heavy metal chemical compounds such as uranyl formate. Because the construction of the proteins is in close proximity to the solvent, the contrast between them is usually very faint without such staining. However, this staining is known to result in deformation of the specimen due to dryness and uneven staining<sup>15</sup>. Therefore, these effects have been determined to limit the resolution of analysis at around 20 Å. In spite of these unfavorable effects, negative staining remains a common method. In fact, important techniques including low dose conditions and the defocus contrast method have been developed based on this framework.

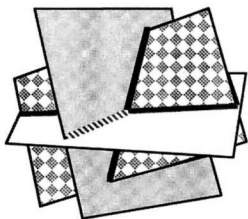
Another approach observes a replica of the specimen with heavy metal coating. Since metal replicas are more stable for electron



(a)



(b)



(c)

**Fig. 1.** Angular reconstitution using common line theory. (a) If a projection image is integrated along a line on the projection plane, a common line exists between two different projection images which corresponds a certain vector in object space. Two individual image profiles are identical on those common lines. Therefore, the two images will intersect on those common lines. (b) With three sets of projected densities, there are pairs of common lines for the other two images. Those three projection angles can be determined through the arrangement to fit those common lines among them(c).

microscopy, it achieves a higher signal-to-noise ratio. Rotary shadowing, an experimental technique, has been developed as a generally feasible protocol. On the other hand, it is accompanied by unfavorable particle enlargement and artificial noise. However, although this method reveals only the molecular envelope, it allows observations of structural changes and interactions with other molecules. Additionally, *in vivo* tissues can also be observed by using quick-freeze deep-etch replicas<sup>16</sup>.

## Computer image processing

The first step of the image processing starts by digitizing a micrograph recorded on conventional film using a scanner with high definition optics. Required conditions are, for example, the scanning steps of <20 µm and a dynamic range of ~10<sup>4</sup> for the gray scale. Therefore, image processing systems are also required to handle pixel data in floating point numbers or 16 bit integers. Besides film recording, modern image recording equipment with CCD area detector for applications in electron microscopy are available. However, micrographs recorded on film provide confirmed accuracy with sufficient spatial resolution.

Next, a series of particle images are sampled from micrographs. Using an interactive computer program, hundreds of particles are picked up in a micrograph manually. This, however, is a tedious and time-consuming task. There had been trials for automated particle pickup systems, but a trivial particle recognition algorithm quickly fails unless the particle is distinct enough, especially in the case of single protein molecules. The algorithms for picking up particles are subtle and are expected to be explored through the use of artificial intelligence.

## Contrast transfer function

Because organic materials such as proteins are very low contrast in electron microscopy, they are observed under defocus conditions in order to enhance the contrast. It usually reaches more than several thousands Å, therefore, the image formation involved in microscopy is always accompanied by modulation. Without this correction, the resolution of electron microscopy is known as the Scherzer limit.

The effect was known as the contrast transfer function (CTF) derived through the weak phase approximation in the elastic scattering<sup>12</sup>. Intuitively, it defines how a single point looks spread in the image. In the Fourier transform of the observed image, the CTF is

multiplied in its spatial frequency component. Therefore, it consists of phase contrast and amplitude contrast. The phase contrast comes mostly from spherical aberration, which is a characteristic of the electric lens. The amplitude contrast is affected by many factors, one of which depends on the thickness of the specimen. While amplitude contrast correction is treated in the 3D reconstruction, phase contrast correction is required before analysis for the proper comparison of two images in different defocus conditions. In practice, actual defocus value in each micrographs have to be determined first. Calculating the Fourier transform of the image, the circular modulation of the image's spatial frequency component represents phase contrast effects, known as the Thon ring. From its sinuous modulation, defocus values are determined. Phase contrast is then corrected by a filter to compensate for phase flipping in certain spatial frequency components by the CTF.

## Alignment of observed particle images

Due to the low dose condition which minimizes radiation damage, the observed particles are immersed in background noise. Averaging images in the same orientation is the primary noise reduction method. Therefore, similar images are scanned for position shift and rotation repeatedly in order to fit an image.

Well determined particle images in a micrograph can provide representative images of particles in various orientations as a reference, though this constitutes a pitfall if one prefers some reference particle images that can potentially yield an proposition which might deviate from the genuine structure. Therefore, reference free alignment addresses this problem by trying to extract common patterns among numerous images of particles<sup>5,17</sup>. In general, the orientation of the particle in 3D space is defined in terms of three variables, usually in Euler-angles. The in-plane rotation of images should be aligned first, resulting in two undetermined variables for the particle direction.

The principal component analysis, known as a multivariate statistical analysis, has been introduced in order to distinguish groups of similar images. Since images are already aligned rotationally, pixel data can be directly evaluated using eigenvalue mathematics. In particular, the corresponding analysis is preferred for the scale invariant comparison of the image data set. Obtained clusters will provide appropriate groups corresponding to the 2 direction angle variables as well as other factors of those images.

When electron microscopy images are very noisy, the resulting clustering is sometimes unfavorable. In addition, a signal from some

important characteristics of the structure might be too weak to analyse in current methods. Therefore, a combination of the algorithms and heuristic screening procedure is sometimes necessary. For example, hierarchical descendent clustering is another method of finding groups of images in a ‘bottom-up’ manner<sup>18</sup>. Although different clustering algorithms have been developed using limited computational resources, a novel method that takes advantage of modern high performance computers is still required<sup>19</sup>.

Even the first generation clusterings have unfavorable biases to introduced preferences, and are subject to refinement in subsequent 3D reconstruction. Obtained image members in the same group are aligned with each other to form the class average with less noise. They are called ‘characteristic views’, a representative set of images observed in different orientations.

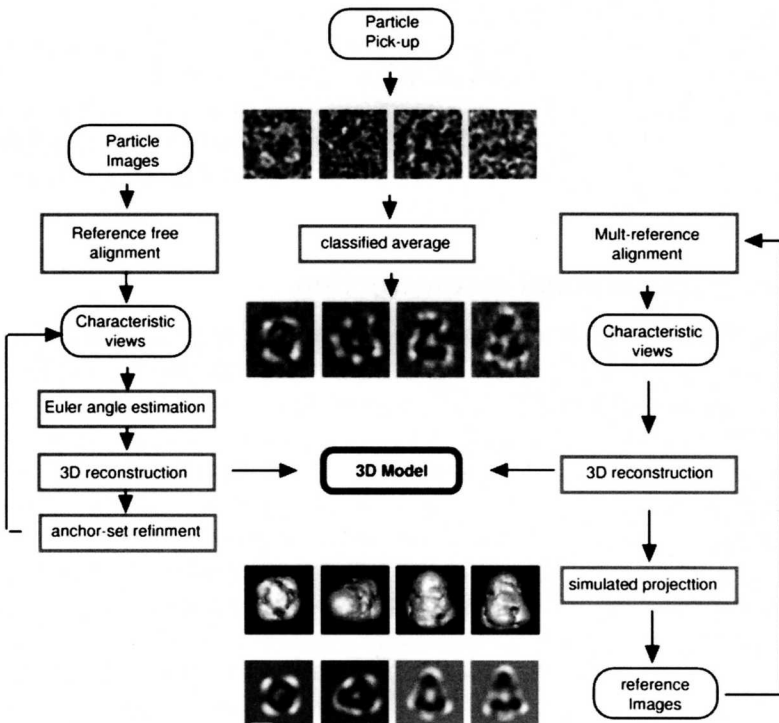
### Three dimensional reconstruction

The characteristic views of the particle obtained are considered projections of the 3D density function, a Radon transform, which is a subject of computer tomography<sup>13</sup>. These projections participate in the 3D Fourier space, which is considered as the structure factor. The back projection is a reverse Fourier transform to reconstruct the 3D structure using sufficient data in Fourier space. The problem with 3D reconstruction for the particle with random orientation is that their projection angle is unknown. Therefore, we have to determine the projection angle and shape simultaneously based on observed images. Earlier, this difficulty was avoided by using a method called ‘random conical tilt’. This method takes micrographs from more than two different tilt angles, which contain film particles with the same faces upward. Intuitively, it is analogous to stereoscopic observation by two eyes. However, this method enforces some prerequisites both for specimens and the tilting stage equipment for the microscope. Furthermore, structural information perpendicular to the specimens’ face becomes blurred. This is called the ‘missing cone’ problem, which involves a lack of structure factor in the conical region of the Fourier space.

Therefore, an angular reconstitution method has been proposed based on particle images in random orientation<sup>5</sup>. This method also raised challenges regarding the computational solution for estimating the particle orientations based on noisy images. The reported successful results were based on the common line theorem for the projected images. Using angular reconstitution, we can make greater use of the ice-embedded specimen while retaining the native protein structure through the use of cryo-electron microscopy.

The principle of projection angle estimation relies on the fact that the two projected images in different orientations share a line of the three-dimensional object (Figure 2). The common line theorem ensures that the unique line exists for the pair of images where the

#### The angular reconstruction



#### The projection matching

**Fig. 2.** Angular reconstitution (left side) and projection matching (right) in the three-dimensional reconstruction. Collected particle images are initially classified in terms of a reference-free alignment. The class averages then provide the first characteristic views. Angular reconstitution is a method for estimating Euler-angles for those projection images, and the 3D reconstruction provides the first 3D model. Next, projection matching refines the 3D reconstruction. Using simulated projection images at various Euler-angles, the multi-reference alignment collects raw images close to them. A new set of classified averages and a refined 3D model are then obtained. Thus, projection matching iteration refines both classification and 3D model. Anchor-set refinement in the angular reconstitution is in fact another projection matching iteration designed to refine the center positions and Euler angles for characteristic views (modified from Nature, 409: 1047–1051, 2001).

density profiles along those lines become identical. Therefore, characteristic views are investigated for candidates of common lines. First, one-dimensional density profiles at various angles are calculated for a characteristic view, that is called a ‘sinogram’. Then, an agreement between two sinograms, a cross-sinogram, gives an estimate of the best matching common line. Since sub-optimal scores may contribute to a consensus arrangement for multiple projection images, the estimation process becomes a global optimization problem of common lines for the set of characteristic view<sup>20</sup>.

Once projection angles are assigned to the characteristic views, the back projection can be applied to reconstruct a three-dimensional density map of the particle. Although the first reconstruction based on characteristic views is crude, it provides a tentative model of the observed motif for the projected images. Then the reconstruction proceeds in its iterative refinement.

## Refinement by projection matching

What we expect in the 3D reconstruction is that the nature of projected images from homogeneous particles will lead us to resolve a unique self-consistent arrangement of the genuine 3D structure. In other words, re-projection of the obtained 3D structure must fit the observation. Taking advantage of the characteristics of the projection, we can refine a reconstructed 3D structure iteratively consistent with the observation.

The projection of the first 3D model provides simulated characteristic views with known projection angles. Employing them as reference images, images close to those references are searched for in raw images and collected. This task is called multi-reference alignment, which creates a classification consistent with that of the 3D model. In addition, their projection angles are already assigned with great accuracy. Therefore, iterating this ‘projection matching’ leads to a consistent 3D density model<sup>17</sup>. Intuitively, this method is similar to the use of a 3D reference structure on the target particle. It assumes a set of particle images which should be observed, then the reference motif of the model is extracted from observed images. The model is refined until it becomes consistent with the observed characteristic views.

Therefore, the subsequent reconstruction will require only consistent images while rejecting malignant data as compared with the constructed model. However, some inconsistent images and artifacts in the first classification of the observed image do not always create misleading results, but become a subject for refinement. The cluster-

ing of images are resumed in the iterative 3D reconstruction trying to improve clustering based on the reference 3D model. It has some similarities to the initial phasing in X-ray protein crystallography, which might be inaccurate at first, but provides an initial direction for the construction of the electron density map. The precise phase is then determined by calculations using an atomic model for the molecule.

Theoretically, this iteration does not always guarantee convergence to a global minimum. It means that we should start from a reasonably correct 3D structure before beginning the refinement process. We can then derive a genuine structure consistent with the observation based on the reference-free protocol.

## Reconstruction assessment

In the angular reconstitution method, estimated Euler-angles are examined for their wide coverage in Fourier space, using a scatter map of Euler-angles. The obtained 3D reconstruction is then examined with regard to volume and resolution. For the protein molecule, the expected volume is calculated based on its molecular weight. In rendering the surface model for the particle, the isosurface value is chosen to give the approximate target volume. In general, smaller volumes will show better structural features. To obtain an accurate volume, the amplitude contrast of the CTF should be corrected, which is also called a volume recovery.

The resolution of the model is evaluated in terms of the agreement of two independent reconstructions. The agreement of the reconstructions is compared in each resolution using formulas such as differential phase residual or Fourier ring correlation. These usually measure conceptually similar statistics, but sometimes disagree. Therefore, different scores such as Q-factor and spectral signal-to-noise ratio(SSNR) are also examined<sup>13</sup>.

## Software packages

Based on software development activities in academic laboratories, software packages are available with tutorial documentation. There are three popular packages: IMAGIC (<http://www.imagescience.de>) is targeted to the angular reconstitution method with projection angle estimation; SPIDER ([http://www.wadsworth.org/spider\\_doc/spider/docs/](http://www.wadsworth.org/spider_doc/spider/docs/)) provides a rich set of programs for the ‘conical tilt series’ method; EMAN (<http://ncmi.bioc.bcm.tmc.edu/~stevel/>

EMAN/doc/) equips ‘projection matching’ for 3D reconstruction with sophisticated user interfaces including CTF parameter estimation. Since resolution improvement is the target in the iterative 3D reconstruction, FREALIGN<sup>21</sup> features projection matching iteration minimizing resolution penalty; it also addresses optimum CTF corrections.

With these well-developed software packages, some current problems in single particle analysis are now open to solutions by means of computer science. The first would be automatic particle pickup after preliminarily particle views are derived<sup>13</sup>. That kind of automation will increase the number of particle images in different orders, *i.e.*, more than 100,000. The second would be a clustering of inhomogeneous particles. These are the samples of partially purified proteins, a mixture of reaction intermediate states, or a complex containing other molecules. The mixture of different structures could be a subject of clustering and classification of the difference. It is noteworthy that we have also found that an interpreted programming language is a useful tool for testing novel algorithms and applications. Semper (Synopitics Ltd., UK) provides that kind of software package with programming language to construct one’s own procedures using hundreds of images loaded into the memory.

## The voltage-sensitive channel protein

The following sections describe our results of the single particle analysis of the voltage-sensitive sodium channel protein. In the nervous system, three types of voltage-sensitive channels are known to operate together in a closely coupled manner to amplify, transmit, and generate electric pulses, *e.g.*, the sodium channel, the potassium channel and the calcium channel. The sodium channel is essential for the generation of action potentials, while the potassium channel regulates membrane potential and plays a significant role in synaptic plasticity. Calcium channels are involved in many different functions, including muscle contraction and secretory processes. While calcium channel antagonists are used as clinical drugs, sodium channels are the molecular targets of local anesthetic drugs and one of the main target proteins of various kinds of neurotoxins<sup>22</sup>. Mutations of the sodium channel protein cause human myotonia<sup>22</sup>, periodic paralysis<sup>22</sup>, and long QT syndrome in the heart<sup>22,23</sup>.

Until recently, little has been known about the structure of voltage-sensitive channels, although the isolation and purification of this membrane protein has been studied extensively. Therefore, structural studies are now expected to give further understanding of the

mechanisms governing voltage sensing and related gating, together with the ion selection mechanism which is illustrated by the crystal structure of the potassium channel<sup>11</sup>.

## Sample preparations of the sodium channel

Purified sodium channel proteins from the electric organs of electric eels were solubilized using a detergent<sup>24,25</sup>. In the case of the negative staining of a specimen, particles were absorbed to thin carbon films rendered hydrophilic by glow discharge in air and supported by copper mesh grids<sup>25,26</sup>. For the ice-embedded specimen, a droplet of protein solution was applied to a holey carbon grid and then frozen by ethane slush cooled by a nitrogen gas<sup>6</sup>.

Immunoaffinity chromatography is an efficient method for protein isolation, but it requires an extensive search for a suitable antibody for purification. In general, once the antibody connects with the antigen, it does not easily release the antigen. The antibody complex also becomes a desirable probe which confirms the observed particles as the target protein. In addition, it also works as a label for the binding site of the antibody, *i.e.*, the C-terminus region, which is useful in determining the cytoplasmic side of the membrane protein.

## The 3D structure of the sodium channel

Our first study employed a negatively stained specimen for electron microscopy<sup>25</sup>. One-thousand-four-hundred selected particle images were aligned and applied to the corresponding analysis. The characteristic views obtained illustrated the first low resolution structure of the sodium channel and its family. In order to improve the resolution resulting in a satisfactory 3D reconstruction, ice-embedded specimens under cryo-electron microscopy were employed. The microscopy used in this study features a sample cooling system using liquid helium and 300 kV acceleration voltage which ensures the highest resolution<sup>6</sup>. The images of the sodium channel are less contrasted, but can be recognized as particles in various orientations (Figure 2). Almost 10,000 particle-images were picked up for the analysis and 3D reconstruction study<sup>8</sup>.

By means of the reference-free protocol for image classification, 240 clusters were obtained. Since the particle has a pseudo-four-fold symmetry, the first 3D reconstruction model was obtained assuming a four-fold symmetry. Then, the subsequent iterative 3D reconstruction refined the model without the imposed symmetry. After several refinement cycles, a stable 3D structure was obtained as seen in

Figure 2. The simulated re-projection on the bottom row from the final structure compares closely with the experimental averages in the second row.

The overall structure is bell shaped with an upper narrower region and lower wider region corresponding to 24% and 47% of the total volume. The middle part in between them, a 30 Å wide horizontal band without peripheral holes, contains 29% of the volume as illustrated by white bars in longitudinal views (Figure 3). These values agree closely with those expected from its amino acid sequence (Figure 4). Therefore, the transmembrane region is probably located in the middle part of this particle. Actually, the transmembrane region consist of highly homologous sequences known as four repeats, which correspond to the pseudo-four-fold symmetry. Furthermore, the C-terminal location determined by the antibody (Figure 5) was the lower wider region which is similar to the layout of the amino acid sequence.

Our results also revealed this protein's novel internal structure. The large internal cavities in the cytoplasmic side connect to four narrow, peripheral, low-density regions in the transmembrane domain, and these low-density regions further connect to another large cavity in the extracellular side. Four small orifices in the half-spherical extracellular structure perforate the protein shell close to

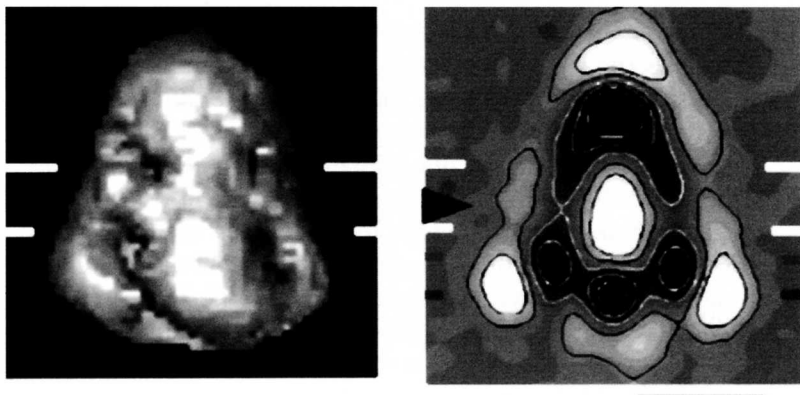


**Fig. 3.** A surface representation of the sodium channel (left) and a cross section along the same face (right). Four small orifices are visible on this surface. A black arrow indicates the constriction between the cytoplasmic (lower) and extracellular (upper) cavities, while bars delineate the lipid bilayer. In the transmembrane region, a central massive body and two peripheral low density regions can be seen. Scale bar, 50 Å (modified from Nature, 409: 1047–1051, 2001).

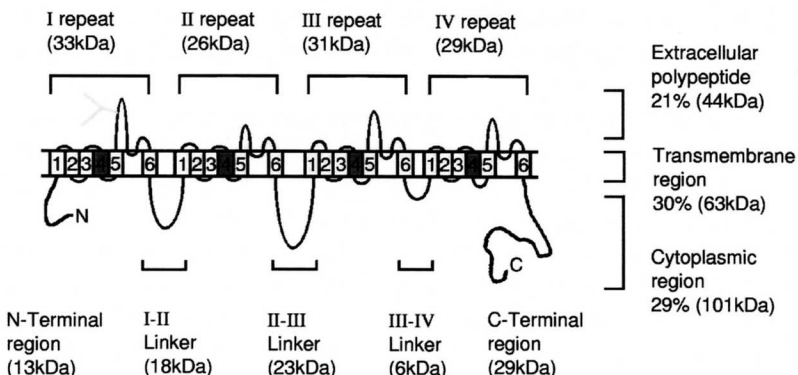


**Fig. 4.** The amino acid sequence and predicted transmembrane regions of the sodium channel. Numbers designate six homologous segments which comprise the transmembrane region. Four segment 4 shown in gray are putative voltage sensors<sup>22</sup> (modified from Nature, **409**: 1047–1051, 2001).

the putative transmembrane region and connect the large internal cavity with the exterior (Figure 3).

## Biological implications

We have postulated that the observed structure of the sodium channel is in a closed state because the opened state of the sodium channel is unstable and usually shifts to stable closed state in a very short period(<1ms). Four peripheral low-density regions form spiral pathways surrounding the central massive body (Figure 3). In these pathways, the narrowest point seems to prevent sodium ions from passing. This model is also in line with the site-directed mutagenesis experiment which concluded the existence of one ion-selective pore in a molecule<sup>27</sup>. In addition, another result suggests that four voltage sensors move to sense the change of the membrane potential<sup>28</sup>. These observations foster the hypothesis that the ion-permeating pathway in the sodium channel will be opened by certain movements of the central massive body into surrounding low-density regions.

Quite recently, the structure of the voltage-sensitive potassium channel<sup>10</sup> and calcium channel<sup>9</sup> have been revealed by single particle analysis using a negatively stained specimen. In the rabbit muscle calcium channel complex, its alpha subunit has a structure similar to the sodium channel. The cytoplasmic side of the alpha subunit was assigned to the larger side<sup>9</sup> in close agreement with the sodium channel<sup>8</sup>. However, another study of the potassium channel structure proposes a potential different-sidedness<sup>10</sup>, which has not yet been

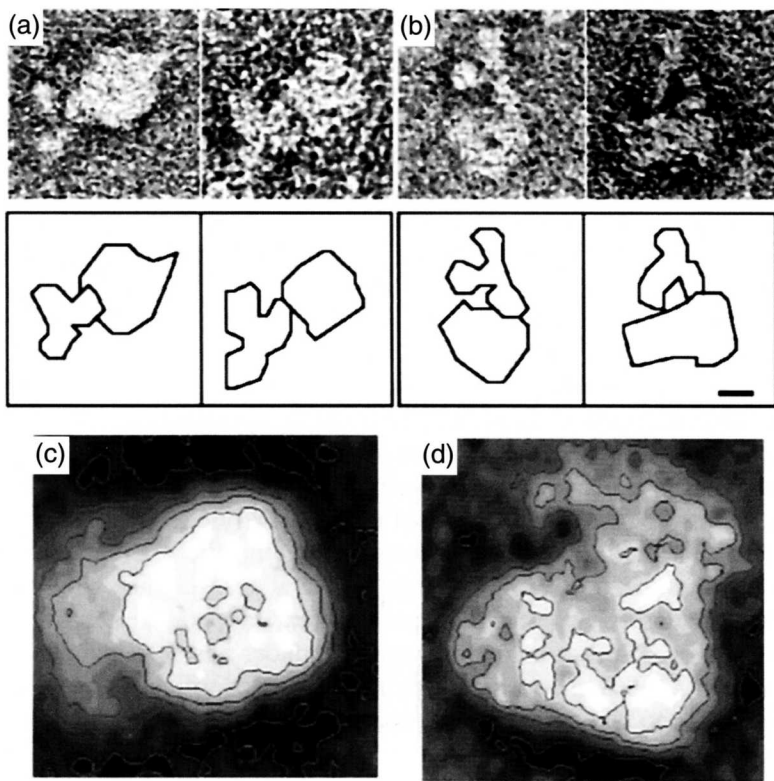


**Fig. 5.** Electron microscopy of negatively stained sodium channel protein-antibody complexes. (a) End-on views; (b) Side views: counters are shown below each row to delineate the antibody and the sodium channel protein. (c) An averaged image of 142 end-on views and (d) one for 76 side views. While the area of flexible antibody is smeared, its binding portion to the protein can be reasonably identified (modified from *Nature*, **409**: 1047–1051, 2001).

ascertained by the probe. Those channel proteins exhibit similar structural features to those of the sodium channel.

## Future directions for single particle analysis

While the molecular mechanisms of protein molecules are ideally understood based on their atomic models, the biological studies, especially for membrane protein, usually proceed without waiting for the result of its crystal structure. In addition, atomic coordinates are sometimes too detailed to provide answers to questions regarding

the protein mechanism. In contrast, the single particle analysis is a more feasible method to obtain low resolution structure of the protein for verification of biochemical knowledge and the hypothesis. In terms of resolution, results regarding icosahedral virus achieved  $\sim 6\text{\AA}$  resolution close to the atomic coordinate<sup>5</sup>. For other specimens without such high symmetry, a further improvement in resolution will require finer imaging in electron microscopy and better statistics. For example, energy filtering electron microscopy is devised to exclude the noise from the inelastic scattering. Furthermore, improvements in clustering images will greatly contribute to the statistical analysis of the particle images.

Single particle analysis in electron microscopy avoids the effect of artificial reagents to label the molecule in spectroscopy, which is sometimes employed in crystallization. Therefore, it is desirable to observe molecular interaction and structural changes directly. For example, the structural changes of the calcium release channel illustrated that global structural changes occur on the opening of the central channel pore<sup>29</sup>. When large structural changes take place in a protein, natural change can be restrained in crystallographic specimens. In addition, if the structural change introduces unstable, fluctuating fragments, NMR spectra does not help atomic coordinate determination. In contrast, single particle analysis provide direct evidence of those events.

Molecular interaction is an another objective of single particle analysis. The interaction of two proteins can be directly observed via electron microscopy, which was also illustrated in antibody binding images. Such molecular interaction is the key to understanding complex molecular systems of membrane proteins. For example, the reaction center protein complex in photosynthesis organism has been reconstructed to reveal the arrangement of their component proteins<sup>30</sup>. Furthermore, advanced reconstruction studies on ribosomes have determined its molecular interactions during peptide synthesis<sup>4</sup>. Although the structures of their component proteins have also been solved by crystallography, analysis of movements in molecular interactions are conceptually problematic in crystallography and NMR. Thus, single particle analysis would play an important role in molecular interaction studies of proteins and biological macromolecules.

## Conclusion

Single particle analysis using electron microscopy allows structural study of protein and biological macromolecules without the need for

special preparations such as crystallization. This method is ideally supported by the cryo-electron microscopy and the angular reconstitution method. It will be reinforced by novel computational methods for automated image pickup, robust image classification, and the detection of inhomogeneous particles. We have demonstrated the first structural analysis of the voltage-sensitive channel using single particle analysis. Underlying molecular mechanisms were discussed in regard to the architectural foundation, which is consistent with many experimental results including the voltage-sensitive gating of the channel. Recent reports concerning single particle analysis indicate that structural resolution has been improving. In addition, its ability to describe structural changes and molecular interactions are other advantages over the crystallography and NMR methods. Thus, single particle analysis meets the current demands of advanced structural studies of proteins and macromolecules.

## Acknowledgments

We express our thanks to Dr Yoshinori Fujiyoshi and Dr Andreas Engel for their illuminating suggestions, and Dr Kiyoshi Asai and Dr Katsutoshi Takahashi for their helpful discussions and software development. This work was supported by a grant from the Japan New Energy and Industrial Technology Development Organization (NEDO).

## References

1. DeRosier, D.J. & Klug, A. (1968) Reconstruction of three-dimensional structures from electron micrographs. *Nature*, **217**, 130–134.
2. Unwin, P.N.T. & Henderson , R. (1975) Molecular structure determination by electron microscopy of unstained crystalline specimens. *J.Mol.Biol.*, **94**, 425–440.
3. Bottcher, B., Wynne, S.A. & Crowther, R.A. (1997) Determination of the fold of the core protein of hepatitis B virus by electron cryomicroscopy. *Nature*, **386**, 88–91.
4. Frank, J. & Agrawal, R.K. (2000) A ratchet-like inter-subunit reorganization of the ribosome during translocation. *Nature*, **406**, 318–322.
5. van Heel, M., Gowen, B., Matadeen, R., Orlova, E.V., Finn, R., Pape, T., Cohen, D., Stark, H., Schmid, R., Schats, M. & Patwardhan, A. (2000) Single-particle electron cryo-microscopy: towards atomic resolution. *Qual Rev Biophys*, **33**, 307–369.
6. Fujiyoshi, Y. (1998) The structural study of membrane proteins by electron crystallography. *Adv. Biophys.*, **35**, 25–80.
7. Serysheva, II, Orlova, E.V., Chiu, W., Sherman, M.B., Hamilton, S.L. & van Heel, M. (1995) Electron cryomicroscopy and angular reconstitution used to

- visualize the skeletal muscle calcium release channel. *Nat. Struct. Biol.*, **2**, 18–24.
8. Sato, C., Ueno, Y., Asai, K., Takahashi, K., Sato, M., Engel, A. & Fujiyoshi, Y. (2001) The voltage-sensitive sodium channel is a bell-shaped molecule with several cavities. *Nature*, **409**, 1047–1051.
  9. Murata, K., Odahara, N., Kuniyasu, A., Sato, Y., Nakayama, H. & Nagayama, K. (2001) Asymmetric arrangement of auxiliary subunits of skeletal muscle voltage-gated I-type Ca(2+) channel. *Biochem. Biophys. Res. Commun.*, **282**, 284–291.
  10. Sokolova, O., Kolmakova-Partensky, L. & Grigorieff, N. (2001) Three-Dimensional Structure of a Voltage-Gated Potassium Channel at 2.5 nm Resolution. *Structure*, **9**, 215–220.
  11. Doyle, D.A., Morais Cabral, J., Pfuetzner, R.A., Kuo, A., Gulbis, J.M., Cohen, S.L., Chait, B.T. & MacKinnon, R. (1998) The structure of the potassium channel: molecular basis of K+ conduction and selectivity. *Science*, **280**, 69–77.
  12. Frank, J. (1992) *Electron tomography: three-dimensional imaging with the transmission electron microscope*. Plenum Press, New York.
  13. Frank, J. (1996) *Three-dimentional electron microscopy of macromolecular assemblies*. Academic Press, Inc., California.
  14. Adrian, M., Dubochet, J., Lepault, J. & McDowall, A.W. (1984) Cryo-electron microscopy of viruses. *Nature*, **308**, 32–36.
  15. Fujiyoshi, Y., Morikawa, K., Uyeda, N., Ozeki, H. & Yamagishi, H. (1983) Electron microscopy of tRNA crystals. I. Thin crystals negatively stained with uranyl acetate. *Ultramicroscopy*, **12**, 210–212.
  16. Katayama, E., Funahashi, H., Michikawa, T., Shiraiishi, T., Ikemoto, T., Iino, M. & Mikoshiba, K. (1996) Native structure and arrangement of inositol-1,4,5-trisphosphate receptor molecules in bovine cerebellar Purkinje cells as studied by quick-freeze deep-etch electron microscopy. *EMBO J.*, **15**, 4844–4851.
  17. Penczek, P., Radermacher, M. & Frank, J. (1992) Three-dimensional reconstruction of single particles embedded in ice. *Ultramicroscopy*, **40**, 33–53.
  18. van Heel, M. (1989) Classification of very large electron microscopical image data sets. *Optik*, **82**, 114–126.
  19. Pascual, A., Barcena, M., Merelo, J.J. & Carazo, J.M. (2000) Mapping and fuzzy classification of macromolecular images using self-organizing neural networks. *Ultramicroscopy*, **84**, 85–99.
  20. Penczek, P.A., Zhu, J. & Frank, J. (1996) A common-lines based method for determining orientations for  $N > 3$  particle projections simultaneously. *Ultramicroscopy*, **63**, 205–218.
  21. Grigorieff, N. (1998) Three-dimensional structure of bovine NADH:ubiquinone oxidoreductase (complex I) at 22 Å in ice. *J. Mol. Biol.*, **277**, 1033–1046.
  22. Catterall, W.A. (2000) From ionic currents to molecular mechanisms: the structure and function of voltage-gated sodium channels. *Neuron*, **26**, 13–25.
  23. Deschenes, I., Baroudi, G., Berthet, M., Barde, I., Chalvidan, T., Denjoy, I., Guicheney, P. & Chahine, M. (2000) Electrophysiological characterization of SCN5A mutations causing long QT (E1784K) and Brugada (R1512W and R1432G) syndromes. *Cardiovasc. Res.*, **46**, 55–65.
  24. Miller, J.A., Agnew, W.S. & Levinson, S.R. (1983) Principal glycopeptide of the tetrodotoxin/saxitoxin binding protein from Electrophorus electricus: isolation and partial chemical and physical characterization. *Biochemistry*, **22**, 462–470.

25. Sato, C., Sato, M., Iwasaki, A., Doi, T. & Engel, A. (1998) The sodium channel has four domains surrounding a central pore. *J Struct Biol.*, **121**, 314–325.
26. Ellisman, M.H., Miller, J.A. & Agnew, W.S. (1983) Molecular morphology of the tetrodotoxin-binding sodium channel protein from *Electrophorus electricus* in solubilized and reconstituted preparations. *J. Cell. Biol.*, **97**, 1834–1840.
27. Heinemann, S.H., Terlau, H., Stuhmer, W., Imoto, K. & Numa, S. (1992) Calcium channel characteristics conferred on the sodium channel by single mutations. *Nature*, **356**, 441–443.
28. Stuhmer, W., Conti, F., Suzuki, H., Wang, X.D., Noda, M., Yahagi, N., Kubo, H. & Numa, S. (1989) Structural parts involved in activation and inactivation of the sodium channel. *Nature*, **339**, 597–603.
29. Orlova, E.V., Serysheva, II, van Heel, M., Hamilton, S.L. & Chiu, W. (1996) Two structural configurations of the skeletal muscle calcium release channel. *Nat. Struct. Biol.*, **3**, 547–552.
30. Remigy, H.W., Stahlberg, H., Fotiadis, D., Muller, S.A., Wolpensinger, B., Engel, A., Hauska, G. & Tsiotis, G. (1999) The reaction center complex from the green sulfur bacterium *Chlorobium tepidum*: a structural analysis by scanning transmission electron microscopy. *J. Mol. Biol.*, **290**, 851–858.